

Stability assessment of a circular earth dam

Ashok K. Chugh^{*,†}

U.S. Bureau of Reclamation, Denver, CO 80225, U.S.A

SUMMARY

Stability of a circular earth dam is assessed for radial cracking potential and static slope stability using continuum mechanics-based three-dimensional numerical models. Comparisons of numerical model results for a circular water tank with vertical walls and different radii with their analytical counterparts are included to support the validity of the ideas and their implementation in the continuum mechanics-based computer program used. Effects of sloping wall faces and Poisson's ratio on computed deformations and stresses are also included. The same numerical models are used to assess stability of a circular dam in terms of factor-of-safety and associated failure surface. Three-dimensional slope stability analysis results are compared with continuum based two-dimensional slope stability analysis results to assess the magnitude of 3D effects. Example problems are included to illustrate the use of ideas presented. Published 2013. This article is a U.S. Government work and is in the public domain in the USA.

Received 4 June 2012; Revised 14 November 2012; Accepted 15 November 2012

KEY WORDS: circular dams; circular reservoirs; curved embankments; cracks; slope stability; two- and three-dimensional analysis

1. INTRODUCTION

Dams are generally constructed in river valleys for water storage, power generation, and for flood control purposes. For these structures, valley walls provide natural end-supports. These dams are generally referred to as water storage dams. There are also off-stream water storage dams, which are constructed in non-valley environments. The off-stream storage dams are self-contained structures (do not have end-supports) and can have a variety of geometric configurations depending on their locale and local landform (topography). These self-contained water retaining structures are called ring dams. A.V. Watkins Dam near Ogden, Utah, and Warren H. Brock Reservoir near El Centro, California, are examples of ring dams. A circular dam is a ring dam of circular configuration. Hyden Humps Dam near Hyden, Western Australia, is an example of a circular dam. Aerial views of these facilities can be seen on the internet using Google Earth or other similar sites. The work included in this paper pertains to circular dams.

In a river valley, an embankment dam can be built with an upstream curve in plan to increase compressive stresses in the dam under the reservoir water pressure [1]. However, in a circular reservoir, the ring dam cannot be arched against the reservoir pressure. In addition, the reservoir water pressure causes hoop tension, which is a tensile stress in the circumferential direction of the dam. In a thick-wall cylinder, internal pressure causes hoop tension, which has maximum value at the inner surface and decreases exponentially across the wall thickness to a non-null tensile stress value on the outer surface; the hoop tension causes development of microcracks, which initiate at the inner surface and propagate radially toward the outer surface [2, 3]. Also, experience with stress analysis of reinforced concrete circular water tanks indicates that, depending on its size, a relatively large proportion of the water

*Correspondence to: Ashok K. Chugh, U.S. Bureau of Reclamation, Denver, CO 80225, U.S.A.

†E-mail: Achugh@usbr.gov

pressure on the tank wall is resisted by hoop tension in the wall. Figure 1 shows the relative proportions of water pressure resisted by hoop tension and that resisted by cantilever action in different size circular tanks [4]. Figure 1 is adapted with permission of the Concrete Society, U.K. It is based on the Reissner's method of calculating restraint in cylindrical liquid storage tanks [5]. Slurry tanks of large diameter designed to resist the liquid pressure by cantilever action only (i.e., ignoring the hoop stress) are known to have actually cracked and leaked badly [4].

Tensile stresses in earth dams are of particular concern as they can affect both seepage and stability of the dam. The reservoir water pressure-induced stresses are to be combined with the stresses because of self-weight of the dam and the pore water pressure to assess the stability of a circular earth dam. Reference [6] provides details about the nature and significance of cracking in earth dams.

The main objectives of this paper are the following:

- (a) identify the presence of tensile stresses or reduced compressive stresses in a circular earth dam;
- (b) assess static slope stability of a circular earth dam; and
- (c) make recommendations for stability assessment of circular earth dams.

To achieve these objectives, the items of interest for circular dam stability are as follows: (a) slope stability, and (b) confining stresses which in turn affect (a). Seepage-related issues, such as increased seepage, internal erosion, and hydraulic fracturing, because of radial cracks or zones of tensile stress or reduced net compressive stress are important but not included in this paper. Similarly, initiation and propagation of cracks in an earth dam are items of interest but not included in this paper.

Assessments of tension zones and cracking potentials in a circular embankment included in this paper are based on linear elastic analyses, that is, all materials are assumed to be perfectly elastic. In 1967, Casagrande had suggested that this assumption of stress-strain properties of materials exaggerates the magnitude of the tensile stresses; it does not significantly change the geometry of the tension zones and the location of the maximum tensile stresses as compared with those that develop in an actual embankment. The hypothesis and its validity are documented by Covarrubias in reference [7], and it was accepted as a matter-of-fact for the work included in this paper. Covarrubias had used finite element method to demonstrate good agreement between the theoretical results and observations on four dams in which cracks or large tension zones had developed. Covarrubias had considered weight of the embankment as the only load in analyses of earth and rockfill dams located in river valley environment.

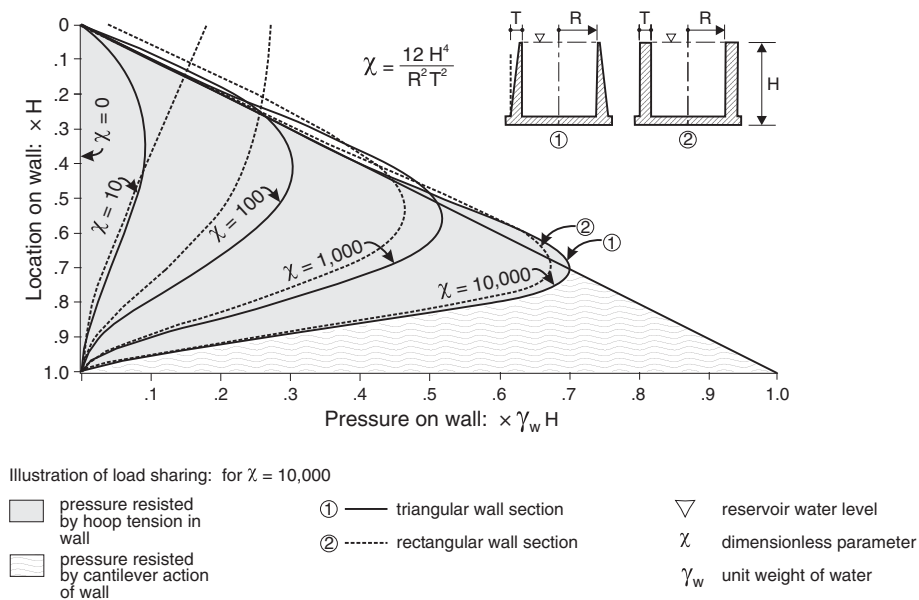


Figure 1. Typical load-distribution curves on wall of cylindrical water tanks, based on Reissner's method [4] — adapted with permission of the Concrete Society, UK.

The computer programs referenced in this paper are FLAC [8] and FLAC3D [9]. FLAC and FLAC3D are acronyms for Fast Lagrangian Analysis of Continua—FLAC is for two-dimensional analysis, and FLAC3D is for three-dimensional analysis. These programs were used for deformation and stress analyses and for slope stability analyses; their adoption and use was for convenience. The information presented in this paper can be used in other computer programs that are similar in principle to the ones used herein. References included in this paper are representative but not a complete list of works on the subject.

For ease of presentation, the following conventions are used in this paper:

- (a) Geometry is referenced in Cartesian (x, y, z) and cylindrical (r, θ, z) coordinates; both coordinate systems follow the right-hand rule. Two-dimensional cross section is in xz or rz plane.
- (b) Cartesian coordinates are used in FLAC and FLAC3D computer programs. For ease of interpretation of analysis results, items of interest were transformed into cylindrical coordinates. Information presented in this paper is in terms of both coordinate systems.
- (c) Stresses are referenced using the symbol σ and the convention of face and coordinate direction as subscripts. For example, σ_{xx} refers to normal stress on face x and pointing in the x coordinate direction, σ_{xy} refers to shear stress on face x and pointing in the y -coordinate direction, σ_{rr} refers to radial stress on face r and pointing in r coordinate direction, $\sigma_{\theta\theta}$ refers to circumferential stress on face θ and pointing in θ coordinate direction, $\sigma_{r\theta}$ refers to shear stress on face r and pointing in the θ coordinate direction, etc. A positive face has outward normal vector pointing in the positive coordinate direction; a negative face has outward normal vector pointing in the negative coordinate direction. A positive stress acts on a positive face and points in the positive coordinate direction or on a negative face and points in the negative coordinate direction. According to this convention, tension is positive, compression is negative, and positive shear stress on a positive face points in the positive coordinate direction and on a negative face points in the negative coordinate direction.
- (d) Displacements are referenced using the symbols $u, v,$ and w and refer to displacements in x -, y -, and z - coordinate directions, respectively. In cylindrical coordinates, symbols $u_r, u_\theta,$ and u_z are used to refer to displacements in r -, θ -, and z - coordinate directions, respectively. Positive displacements are in positive coordinate directions; negative displacements are in negative coordinate directions.

2. MOTIVATION

The work included in this paper was motivated by having to assess three-dimensional (3D) effects on computed factor-of-safety (FoS) using two-dimensional (2D) numerical models for potential dam modification issues related to existing earth dams. In the past, based on analyses of ideal slopes (see the cited references for details on the slopes that were analyzed), the 3D effects have been reported to be from 10 to 40 percent improvement in computed FoS over their 2D counterparts, Hungr and Wilson [10]. Similar trends were calculated by Adriano et al. [11] for convex and concave geometries (26 and 50 percent, respectively). These results imply that the computed FoS using 3D analysis is 10 to 50 percent higher than the computed FoS using 2D analysis—depending on the geometry of the slope and end conditions, all else being equal. Hungr and Wilson had analyzed slopes (typically used in comparing accuracy of different methods for computing FoS) curved (straight, concave, and convex) in plan view using 3D limit-equilibrium-based computer program CLARA-W. Adriano et al. had analyzed hypothetical slopes concave, plane, and convex in plan using 3D finite element based procedure implemented in proprietary software. In studying the 3D effects on seepage and stability of flood control levee slopes along meanders in a waterway (concave, convex, and straight in plan), Inci [12] cites a less than 5 percent improvement in computed FoS because of curved geometry. Inci had used axisymmetric and plane strain continuum models in FLAC for analysis and recommended verification of the results via 3D analyses. Using 2D axisymmetric analysis of a curved corner of Aitik tailings dam in Sweden, Ormann et al. [13] identified zones of low compressive stresses in the body of the dam because of its curved geometry;

this raised concerns for seepage and slope stability of the dam for future dam raising. Ormann et al. had used the finite element program PLAXIS for analysis and recommended a 3D analysis for further insight into the stress distributions at the curved corner. None of the geometries included in References [10–13] formed a closed loop, which is typical of a ring dam.

In a general sense, a concave slope is expected to have a higher FoS than its convex counterpart, with the FoS for a straight slope being at the transition between the two, all else being equal. This expectation is based on the geometry of the slope (geometry effect). There is also a material effect—deformation and strength properties of soil and ground water conditions in the slope—which affects performance of a slope. Thus, there are two factors, which suggest a 3D slope stability analysis is warranted: (a) curved geometry; and (b) material variability including ground water and foundation conditions. Both of these factors are considered in the analyses presented herein.

Circular dam geometry was selected for assessing 3D effects because of its unique configuration and availability of analytical basis for comparison of computed deformation and stress results on simplified models. Numerical analyses were performed using 3D models and results compared with their 2D counterparts as suggested in References [12, 13]. Limit equilibrium-based slope stability analyses for the circular dam were not performed because of lack of availability of appropriate software.

3. SYMMETRY AND BOUNDARY CONDITIONS

3.1. Symmetry conditions

Referring to Figure 2, a circular homogeneous dam is symmetric about every diameter (one-fold symmetry). Also, each one-fold symmetric section is symmetric about a radial line, which is perpendicular to the one-fold symmetry diameter (two-fold symmetry). In addition, the z-axis passing through the center of the circular reservoir is an axis of rotational symmetry, that is, a circular homogeneous dam is a solid of revolution obtained by rotating a plane cross section of the dam through 2π radians (360°). Also, reservoir water pressure and seepage conditions are identical in every diameter section assuming no changes in material properties. Thus, there is geometric, material, and loading symmetry in a homogeneous circular dam. The foundation block shown in Figure 2 is square shaped; rotational symmetry of the foundation may be viewed along an inscribing circle and ignoring the regions past the inscribed circle.

For analysis purposes, a circular homogeneous dam can be modeled in four different ways as shown in Figure 2: (a) complete 3D model; (b and c) one-half of the 3D model along the N-S or E-W diameter; (d) one-quarter of the 3D model along the N-S and E-W diameters; and (e) a unit-radian sector. Model (a) requires boundary conditions only for the foundation block (and none for the dam); models (b) to (e) require boundary conditions for the dam and foundation. Models (b), (c), and (d) use the north-south and east-west diameter symmetries and offer convenience in defining the boundary conditions in Cartesian coordinates. Model (e) is a 2D axisymmetric representation of model (a) and requires boundary conditions for the out-of-plane, θ , faces.

The information included in this paper is based on model (a); model (e) results included are for comparison purposes. Model (a) is the most general form and allows for material variability in select portions of the dam, foundation, or ground water (individually or collectively); models (b), (c), and (d) are restrictive forms and require material and ground water symmetry across planes of geometric symmetry; model (e) is a 2D axisymmetric analog of models (b) to (d) and requires 2π radians (360°) symmetry.

3.2. Boundary conditions

Boundary conditions (b.c.) are defined in terms of displacements or surface tractions; displacement b.c. apply to surface grid points; surface traction b.c. apply to exposed faces of zones. In Figure 2, boundaries where b.c. need to be defined are identified as boundary plane (bp) and plane of symmetry (ps). For example, referring to Figure 3(c), the $u=v=w=0$ b.c. is for the xy plane representing the bottom face of the foundation block; $u=0$, $v=0$ b.c. apply to yz and xz planes

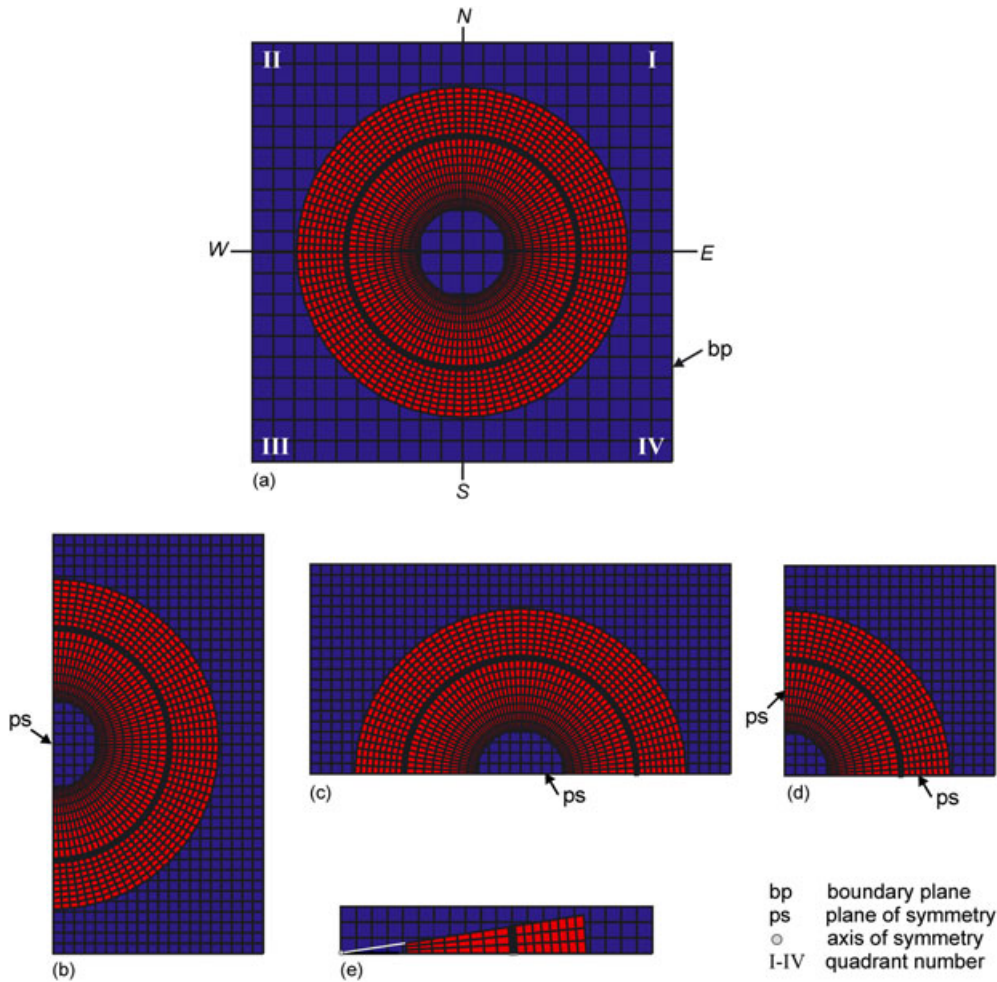


Figure 2. Symmetry conditions, (a) complete model, (b) one-fold symmetric model, (c) alternative one-fold symmetric model, (d) two-fold symmetric model, and (e) axisymmetric model.

representing the end faces of the foundation block in the x - and y -directions, respectively. However, along planes of symmetry in Figures 2(b) to 2(d), the boundary conditions indicated apply to the dam and foundation.

For the axisymmetric model shown in Figure 2(e), the plane cross section is defined in the x - z plane, and the prescribed b.c. of $u = w = 0$ is for the bottom of the foundation block, and $u = 0$ is for the end of the foundation block in x -direction. The axisymmetric model is a unit-radian wide sector in the θ direction centered at the axis of symmetry, and the implied boundary conditions at the two out-of-plane end faces of the unit-radian sector are that of plane strain ($v = u_\theta = 0$).

Because of their uniqueness, application of reservoir water pressure on the inside face of the dam and bottom of the reservoir and application of pore water pressure (pp) because of seepage through the dam (Figure 3) are described as a part of 3D model generation for the sample problem in Section 4.

4. SAMPLE PROBLEM

Figure 3 shows the sample problem analyzed and the terminology used herein. The sample dam is a 25-m high earth embankment and has a 5-m wide crest. The inside slope is 3H:1V (horizontal over vertical), and the outside slope is 2H:1V. The crest of the dam is at elevation 100 m. The

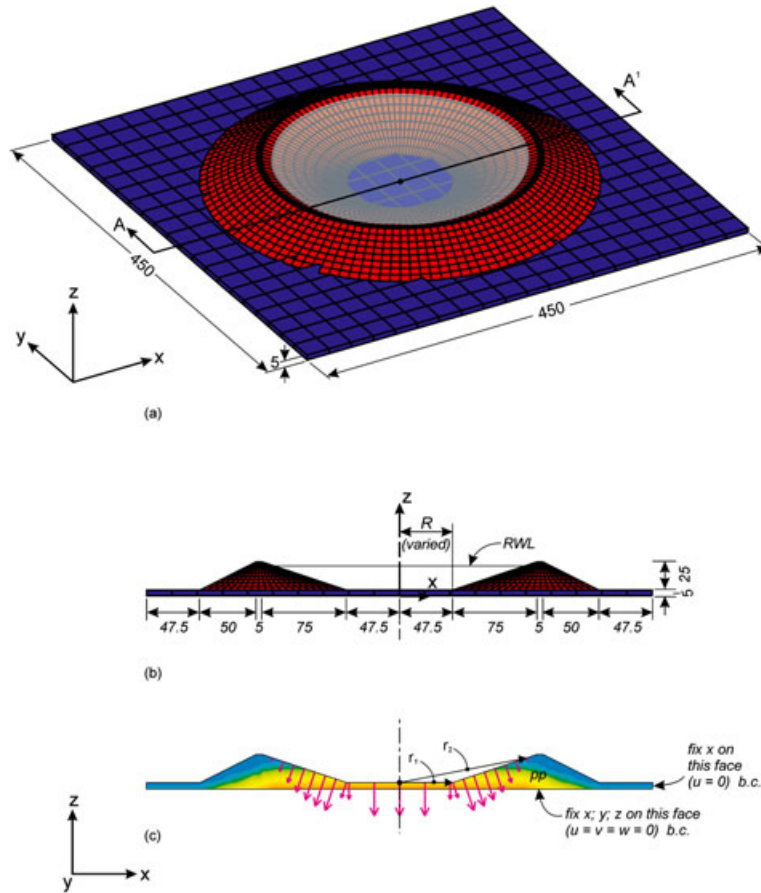


Figure 3. Sample problem, (a) plan view, (b) cross section view, (c) loading and boundary conditions, and (d) model identifications.

reservoir water level (RWL) is at elevation 97 m. The distance from the center of the reservoir to the inside toe of the dam, marked R in Figure 3(b), is varied from 23.75 to 118.75 m in increments of 23.75 m. A 3D model for $R=0$ could not be created because of conflicts in discretization; instead, a model with $R=5$ m was developed to approximate effects of small reservoir on computed responses. Thus, 3D models with $R=5, 23.75, 47.5, 71.25, 95.0,$ and 118.75 m were analyzed. The dam is founded on a 5-m-thick soil-like material, which is underlain by rock. The dam foundation contact is at elevation of 75 m, and the bottom of the foundation block is set at elevation 70 m. The seepage through the dam is assumed to be linearly varying and exiting at the outside toe of the dam.

The dam and foundation materials are assumed to be homogeneous, isotropic, and perfectly elastic-plastic; yield criterion is Mohr–Coulomb; shear flow rule is non-associated, and tensile flow rule is associated. Two sets of soil strength properties for the embankment used are as follows: (a) cohesion, c and angle of internal friction, ϕ ; and (b) c only. For the c only material property (i.e. with $\phi=0$), the Mohr–Coulomb yield criterion becomes Tresca yield criterion; tension limit and tensile flow rule do not apply. Tables I and II show the values of soil properties used; Soil_1 and Soil_2 define the material properties for the dam and foundation, respectively.

All models were developed for the full 3D configuration of the dam, Figure 2(a). Symmetric models shown in Figure 2(b, c, and d) were created by nulling the omitted portions and imposing the applicable boundary conditions at the truncated boundaries. The axisymmetric model shown in Figure 2(e) was analyzed as a 2D axisymmetric model in FLAC. Analyses were performed for determination of the following: (i) elastic deformations and stresses; and (ii) factor-of-safety (FoS) and associated slip surface geometry.

STABILITY ASSESSMENT OF A CIRCULAR EARTH DAM

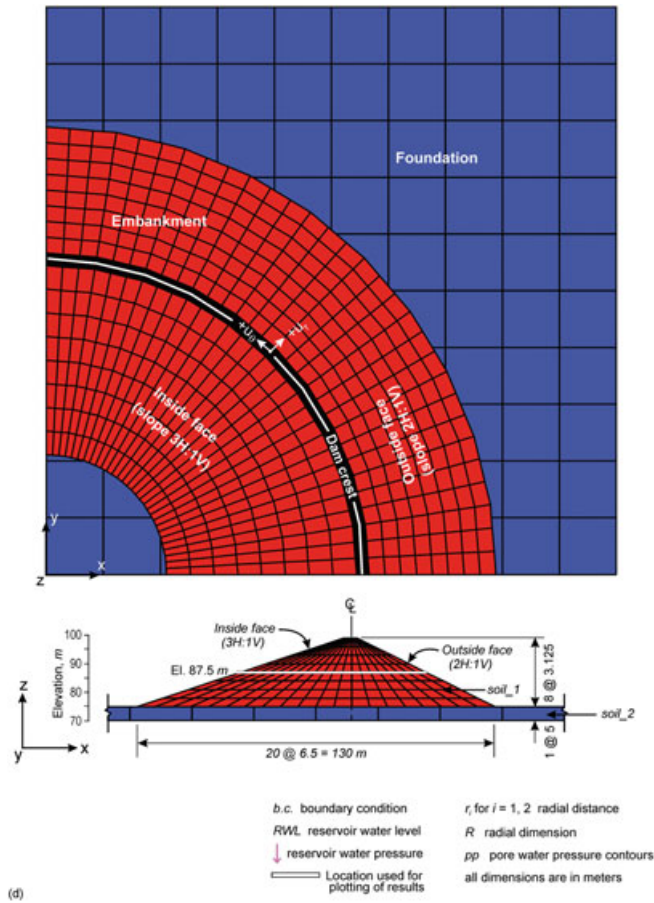


Figure 3. (Continued)

Table I. Material properties set no. 1.

Material	Density	Material strength		Elastic constants	
	ρ (kg/m ³)	c' (kPa)	ϕ' (°)	Bulk modulus (kPa)	Shear modulus (kPa)
soil_1	1850	35	35	1.67×10^4	1.72×10^3
soil_2	2200	500	45	2.50×10^4	2.59×10^3

Unit weight γ (N/m³) = Density \times 9.81.

Table II. Material properties set no. 2.

material	Density	Material strength		Elastic constants	
	ρ (kg/m ³)	c' (kPa)	ϕ' (°)	Bulk modulus (kPa)	Shear modulus (kPa)
soil_1	1850	70*	0	1.67×10^4	1.72×10^3
soil_2	2200	500	45	2.50×10^4	2.59×10^3

Unit weight γ (N/m³) = Density \times 9.81.

*Undrained shear strength.

4.1. 3D model generation

A 3D model for the embankment dam and its foundation is created as two separate units. Each unit is created using a series of 2D planar cross sections (in xz plane) along the y -coordinate direction. At the end, the dam and foundation units are attached to form a single grid. This procedure is similar to the one described in Chugh and Stark [14]. For the circular dam, the following steps were adopted:

- (a) The origin of coordinate system is located at the center of the reservoir. The dam cross section is considered to lie in the xz plane. The foundation and the dam extend in y -direction.
- (b) The foundation is taken to be a cube, which is defined by joining two 2D cross sections in xz planes, y -distance apart, to form a 3D solid. The 3D solid is subdivided into desired number of sub-elements by specifying the number of zones in each of the 3-coordinate directions. For the foundation block shown in Figure 3, the two xz plane sections are 450 m apart in the y -direction, and the region is subdivided into $20 \times 20 \times 1$ sub-elements in the x , y , and z directions, respectively.
- (c) The trapezoidal cross section of the dam is defined in the xz plane at $y=0$. The x , y , z coordinates of a point on the dam cross section located at an angular distance θ from the x axis are calculated using $x=r \cos \theta$, $y=r \sin \theta$, $z=z$ coordinate transformation. Consecutive cross sections are joined to form 3D brick elements. Each brick element is subdivided into desired number of sub-elements by specifying the number of zones in each of the 3-coordinate directions. For the embankment shown in Figure 3, $\theta=9^\circ$ and each 9° increment sector is subdivided into $20 \times 3 \times 8$ sub-elements in the x , y , and z directions, respectively.¹
- (d) In using the coordinate transformation in step (c), θ is incremented continuously in increments for successive planar cross sections of the dam. The periodic nature of sine and cosine functions automatically assigns the appropriate positive (+ve) and negative (-ve) signs to the computed x -coordinate and y -coordinate; the z -coordinate remains unaffected in this transformation.

4.2. 3D model loading

Reservoir water pressure is a traction boundary condition for the inside face of the dam and the positive face of the reservoir bottom, Figure 3(b). For the circular reservoir, the following steps were adopted:

4.2.1. Dam face. The inside face of the circular dam is uniquely identified as being a surface common to the embankment, foundation, and annulus of a sphere with center at the center of the reservoir floor (elevation 75 m) and radius = r_1 and r_2 as shown in Figure 3(c). Reservoir water pressure is applied as a uniformly varying normal stress to the identified dam face.

4.2.2. Reservoir floor. The bottom of the reservoir is uniquely identified as being a surface common to horizontal plane at the bottom of the reservoir and a cylinder with its axis at the center of the reservoir and radius = r_1 as shown in Figure 3(c). The reservoir water pressure is applied as a constant normal stress to the identified floor face.

4.2.3. Seepage pressure. Seepage pressures in the dam and foundation were defined via pore water pressures in these materials. For the circular dam layout, the following steps were adopted:

- (a) Draw the embankment and foundation cross section in xz plane;
- (b) Sketch in the phreatic line;
- (c) Divide the phreatic line into a reasonable number of segments;
- (d) Locate the center of each segment;
- (e) Assign the pore water pressure to all zones below each of the segments as a uniformly varying water pressure.

5. TEST PROBLEM

To gain confidence in the proper functioning of the numerical model set-up and the computed results for the sample problem, it was considered essential to adapt the numerical model of the sample

¹Subdivision of solid elements between consecutive defined sections is in equal parts in the Cartesian coordinates, not in cylindrical coordinates.

problem to a problem with similar characteristics (shape and boundary conditions) and known analytical solution. A circular water tank problem was selected to serve as a test problem. Analytical formulation for lateral deflection of wall of a circular water tank with vertical wall faces and null freeboard, self weight, and Poisson’s ratio (ν) condition is given in Reference [4]; it is in the form of a fourth-order ordinary differential equation and includes its general solution, also see Article 118 in reference [15]. Because stress and strain are proportional for elastic material, the deflected shape of the wall represents, to some scale, the hoop tension at all levels. These criteria were used to validate the correct functioning of the model set-up and to gain confidence in the numerical model results for the sample problem.

5.1. Test problem with vertical wall faces

Figure 4 shows the numerical model for a circular water tank, which was created by assigning 0H:1V slopes to the sample problem geometry. The test problem was assigned the following dimensions: $H=25$ m, $T=5$ m, and $R=5; 23.75; 47.5; 71.25; 95.0,$ and 118.75 m; the wall material was assigned $E=5000$ kPa and $\nu=0$, and the foundation block was assigned $E=7500$ kPa and $\nu=0.45$. Applied pressure on the tank wall and floor correspond to 22-m depth of water. For numerical model results, gravity and pp in the model were set to zero in analysis.

5.1.1. Analytical model results. The analytical solution uses a dimensionless parameter, $\beta = H/\sqrt{R T}$. The results presented in Figure 1 use a dimensionless parameter, $\chi = 12 H^4/R^2 T^2$. Thus $\chi = 12 \beta^4$.

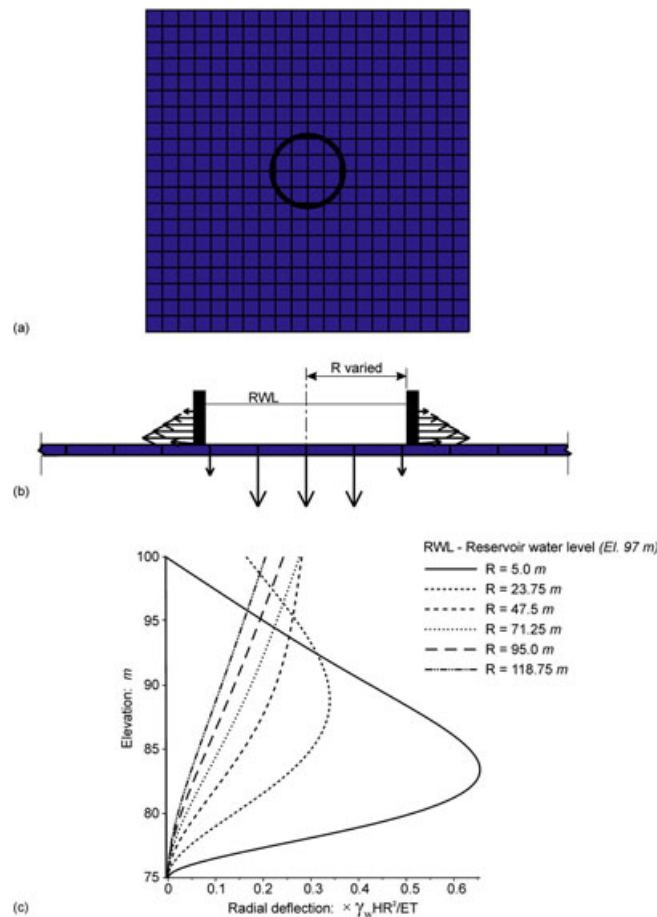


Figure 4. Test problem with vertical wall faces—analytical and numerical model results: loading condition: reservoir water pressure, null self weight, and null pore water pressure, (a) plan view, (b) cross section view, (c) analytical model results, and (d) numerical model results.

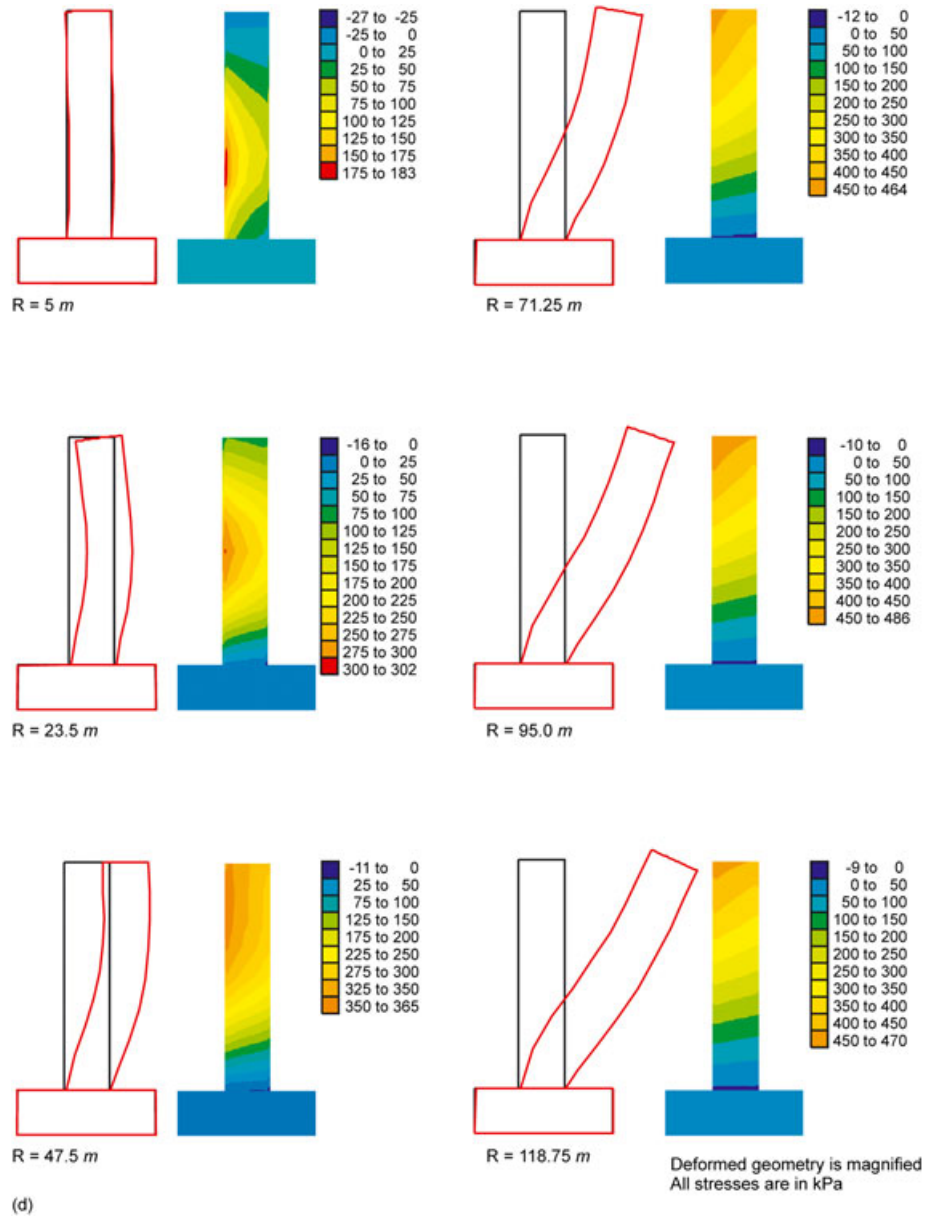


Figure 4. (Continued)

Table III lists the values of β and χ for the test problem dimensions. Results for the analytical solution of the test problem are shown in Figure 4(c).

5.1.2. *Numerical model results.* The numerical model results (deformation and hoop stress contours) are shown in Figure 4(d). Significant observations from comparing the numerical model results with their analytical counterparts include the following:

- The deflected shapes of the wall from the numerical and analytical models compare well; the magnitude of deformations is large because of low value of E used in the calculations ($E = 5000\text{ kPa}$).
- The location of maximum hoop tension matches well with the location of maximum radial deflection;

Table III. Values of dimensionless parameters for the test problem.

Tank radius, R	β	χ
m	(Analytical solution [4])	(Figure 1)
5	5.0	7500
23.75	2.29	332
47.5	1.62	83
71.25	1.32	37
95.0	1.15	21
118.75	1.03	13

- (c) For $R = 118.75$ m or $\beta = 1.03$, the maximum outward deflection and the maximum hoop tension occur near the top of the wall where the water pressure is null;
- (d) For $R < 118.75$ m or $\beta > 1.03$, the locations of maximum outward deflection and the maximum hoop tension successively shift in unison towards the bottom of the wall;
- (e) For $R = 5$ m or $\beta = 5$, the maximum outward deflection and the maximum hoop tension occur towards the bottom of the wall;
- (f) For the test problem data, the maximum hoop tension occurs on the inside face and decreases towards the outside face of the wall.

In view of Figure 1, the results shown in Figure 4(c and d) are interpreted to infer the following: for a given H and T , circular configuration of a water tank (fixed against translation and rotation at the base) provides an inherent circumferential restraint against radial displacement at the top of the tank; the magnitude of this restraint is maximum when R is the least (small radius tank) and decreases rapidly as R gets larger (large radius tank). The inherent restraint is in the form of hoop strap. This explanation is helpful in assimilating the numerical and analytical results shown in Figures 1 and 4.

5.2. Test problem with sloping wall faces

The test problem model with $R = 47.5$ m ($\beta = 1.62$) was selected to assess the effects of Poisson's ratio and sloping wall faces on computed deflections and stresses. The wall slopes were set at 0H:1V and 1H:1V. Each of these models was analyzed for $\nu = 0, 0.25$, and 0.45 . The results of numerical models are shown in Figure 5 and include the wall geometry and the variation of normal and shear stresses through the cross section near mid-height (elevation 86 m), see Figure 3(d).

5.2.1. Analytical model predictions. The analytical results shown in Figure 1 are used as a reference. For $\nu > 0$, $\chi = 12(1 - \nu^2)H^4/R^2 T^2$ [4]. For the test problem with $R = 47.5$ m, $\chi = 83$; thus the plot for $\chi = 100$ is used as a reference. The following are interpreted analytical predictions for the test problem conditions: (1) for a given wall cross-section, hoop tension in the wall should decrease with increase in ν —the rationale being: for $\nu > 0$, χ will decrease, which implies that less of water pressure is resisted by the hoop tension and more is resisted by cantilever action. This suggests that hoop tension should decrease and wall deflection increase with increase in Poisson's ratio. (2) for a given ν value, hoop tension in the wall with sloping faces should be lower than in the wall with rectangular cross section—the rationale being: with larger cross section, the wall deflection will be less, which in turn indicates the magnitude of hoop stress should be less.

5.2.2. Numerical model results. The numerical model results for the two wall slope cases are shown in Figure 5. Significant observations from comparing the numerical model results with the analytical predictions include the following:

- (a) Results shown in Figure 5 agree with the analytical predictions (1) and (2), which are based on the results shown in Figure 1.

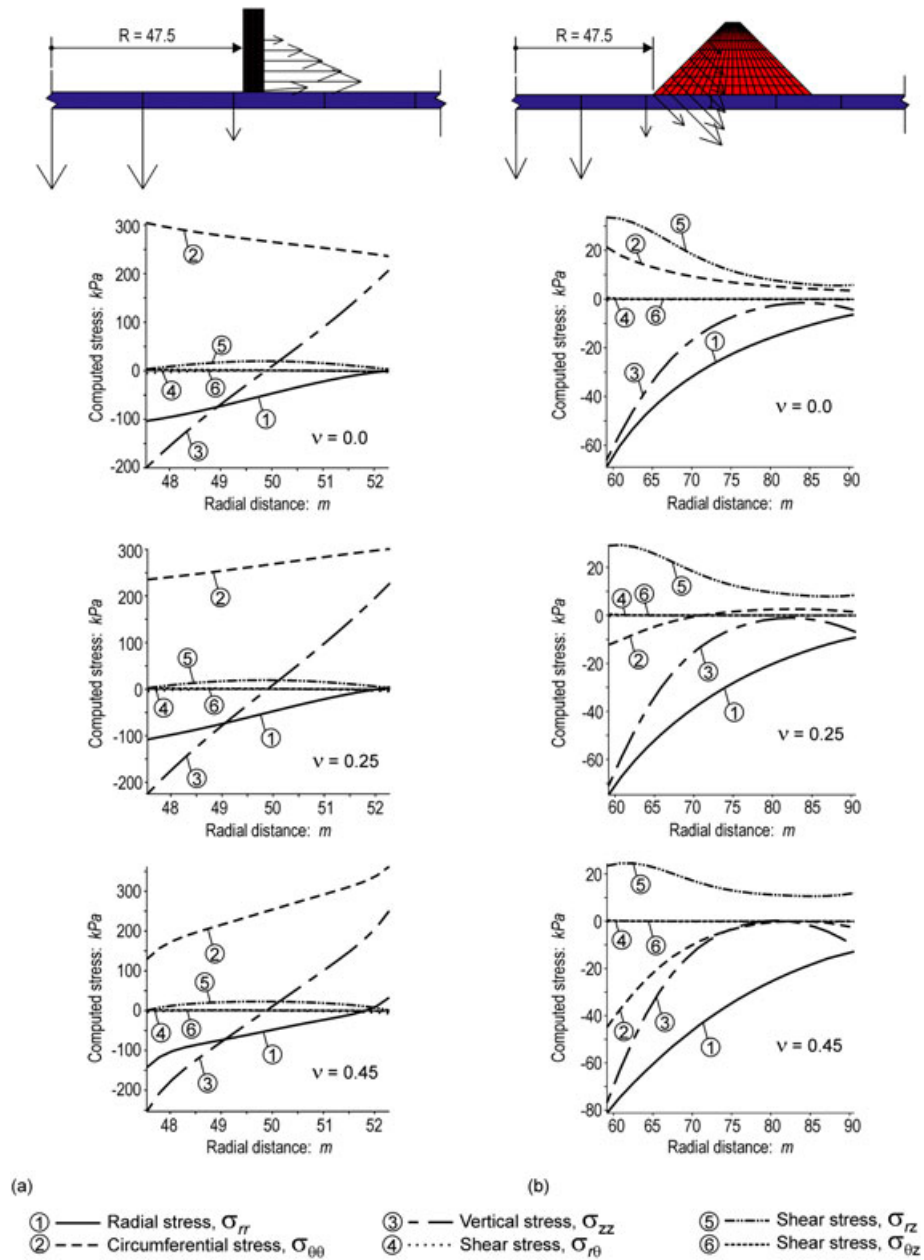


Figure 5. Test problem with sloping wall faces—numerical model results: loading condition is: reservoir water pressure, null self weight, and null pore water pressure, (a) 0H:1V slopes for inside and outside wall faces, and (b) 1H:1V slopes for inside and outside wall faces.

(b) For a given wall cross section, the computed radial deflections increased with increasing Poisson's ratio. However, plots of deformed configurations are not included in Figure 5 to maximize the display of stress results shown and to conserve space.

Results of the test problem give confidence in the validity of the numerical model in determining deformations and stresses, and the procedure was used with confidence in determining tension zones and cracking potentials in the sample problem. In addition, it is learned that the wall cross section geometry and ν are important parameters to understand stress distributions caused by water pressure. The reservoir water pressure-induced stresses are to be combined with the stresses caused by self-weight of the dam and the pore water pressure to assess the location and extent of tension zones in

the sample problem. Thus, a problem-specific analysis using its particular geometry and material properties is included in Section 6.

6. SAMPLE PROBLEM—TENSION ZONES ASSESSMENT

The sample problem with $R = 47.5$ m, 3H:1V inside face slope and 2H:1V outside face slope was selected to assess stresses in the circular dam cross section, see Figure 3. Elastic analyses were performed for the following loading conditions: (a) self-weight of the dam; (b) reservoir water pressure; and (c) self weight of the dam, reservoir water pressure, and seepage induced pore water pressure. For each of the loading conditions, $E = 5000$ kPa, $\nu = 0, 0.25, \text{ and } 0.45$ for the dam; and $E = 7500$ kPa, and $\nu = 0.45$ for the foundation materials were used for the material properties. Thus, for each loading condition, the numerical model was analyzed three times—one per ν value. Poisson's ratio of 0.0, 0.25, and 0.45 were used to better understand the deformations and stresses in a circular dam caused by each of the three loading conditions individually and collectively. In addition, the results for $\nu = 0.0, 0.25, \text{ and } 0.45$ provide a scale by which one can estimate the sensitivity of results to this parameter.

Results for loading condition (a) are useful for a dry circular reservoir; results for loading (a) and (b) combined are useful for a circular dam with an impervious liner, and results for loading condition (c) are useful for a circular dam without an impervious liner. Results for loading condition (b) in itself are considered as an extension of the effects of sloping wall faces on reservoir-induced deformations and stresses included in Section 5.2 and are helpful in understanding results for the loading condition (c).

For assessment of tension zones, the analysis results for each of the three loading conditions are presented using principal stress plots in the dam cross section. The most compressive principal stress is identified as major principal stress, the least compressive principal stress as minor principal stress, and the third principal stress as intermediate principal stress. In the plots showing variation of displacement and stress components across the dam cross section near mid-height of the dam, the displacements are for the nodal points at elevation 87.5 m, and stresses are at the centroids of zones between elevation 84.375 and 87.5 m, see Figure 3. It should be noted that transition from maximum tension to maximum compression is gradual and implies portions of the dam with reduced compression stresses (low confinement).

6.1. Results for self-weight loading condition

The numerical model results are shown in Figure 6 for each of the three ν values used. Significant observations from the results include the following:

- (a) Tension zones occur in the dam cross section for each of the three values of ν .
- (b) Tension zones are located near the top of the embankment and extend down along the sloping faces.

6.2. Results for reservoir water pressure loading condition

The numerical model results are shown in Figure 7 for each of the three ν values used. Significant observations from the results include the following:

- (a) Tension zones occur in the dam cross section for each of the three values of ν .
- (b) Tension zones are located near the top and bottom of the embankment and are more pronounced in the outside half of the dam for $\nu = 0.25$ and 0.45. For $\nu = 0$, tension zones are located in the inside half of the dam.

6.3. Results for self-weight, reservoir water pressure, and seepage-induced pore water pressure loading condition

The numerical model results are shown in Figure 8 for each of the three ν values used. Significant observations from the results include the following:

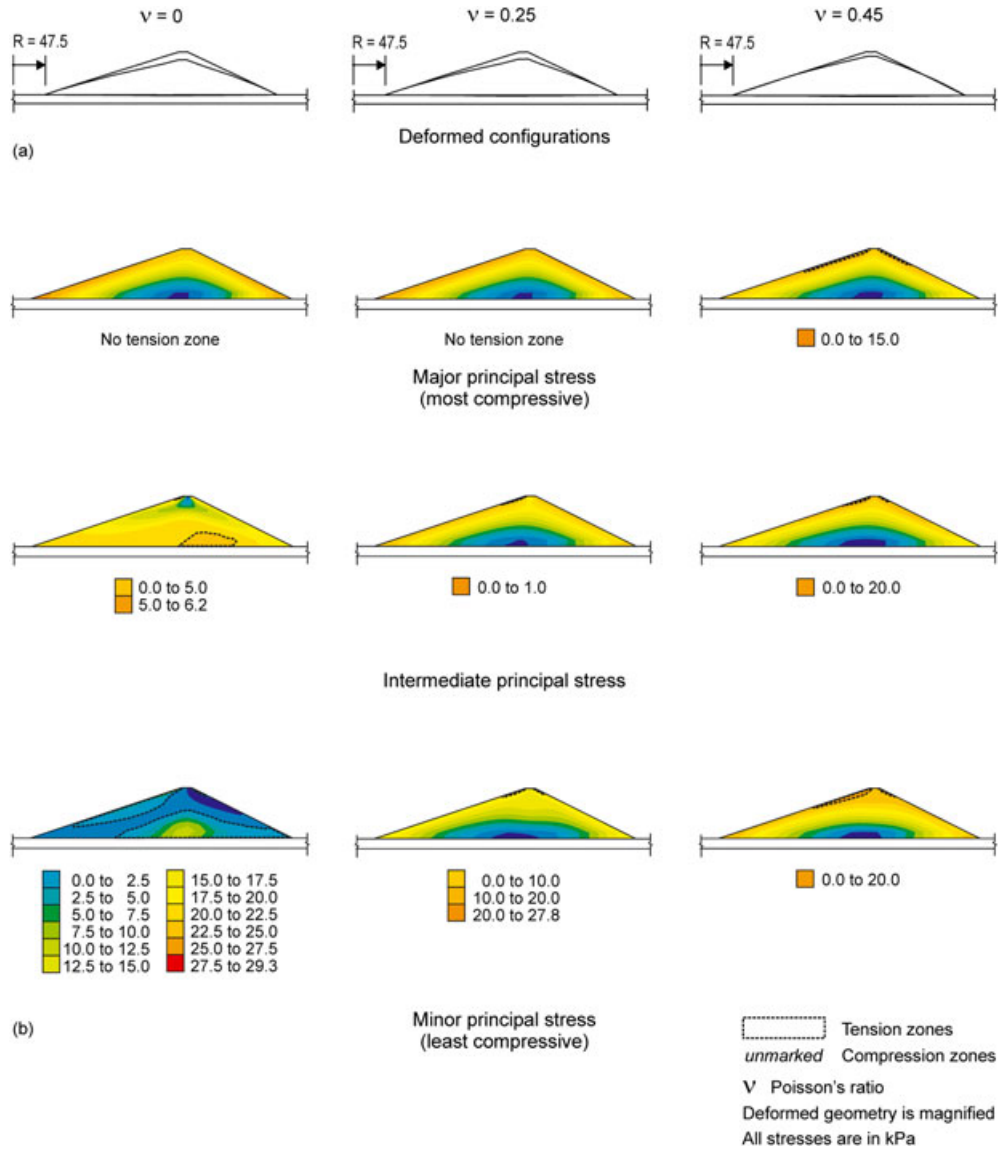


Figure 6. Sample problem (Figure 3); 3D elastic analysis results; loading condition: self weight of the dam, null reservoir water pressure, and null pore water pressure, (a) deformed configuration of the dam cross section, (b) principal stresses in the dam cross section, and (c) displacements and stresses in the dam cross section at mid-height of the dam.

- (a) Tension zones occur in the dam cross section for each of the three values of ν .
- (b) Tension zones are located along the inside face of the embankment and extend well into the inside of the dam.
- (c) Tension zones with the maximum tensile stress are near the inside toe of the dam.

6.4. 2D elastic analysis

The sample problem was also analyzed using a 2D axisymmetric model in FLAC. A plane radial section at $\theta=0$ in 3D model was used in 2D models; the in-plane boundary conditions are the same as in 3D model, and the implied out-of-plane boundary condition for the unit-radian sector in the θ -direction is $u_\theta=0$ for each of the two planes of symmetry, see Figure 2(e). The results for the loading condition (c) are shown in Figure 9 and are in the same format and detail as in Figure 8. Significant observations from the 3D and 2D model results include the following:

STABILITY ASSESSMENT OF A CIRCULAR EARTH DAM

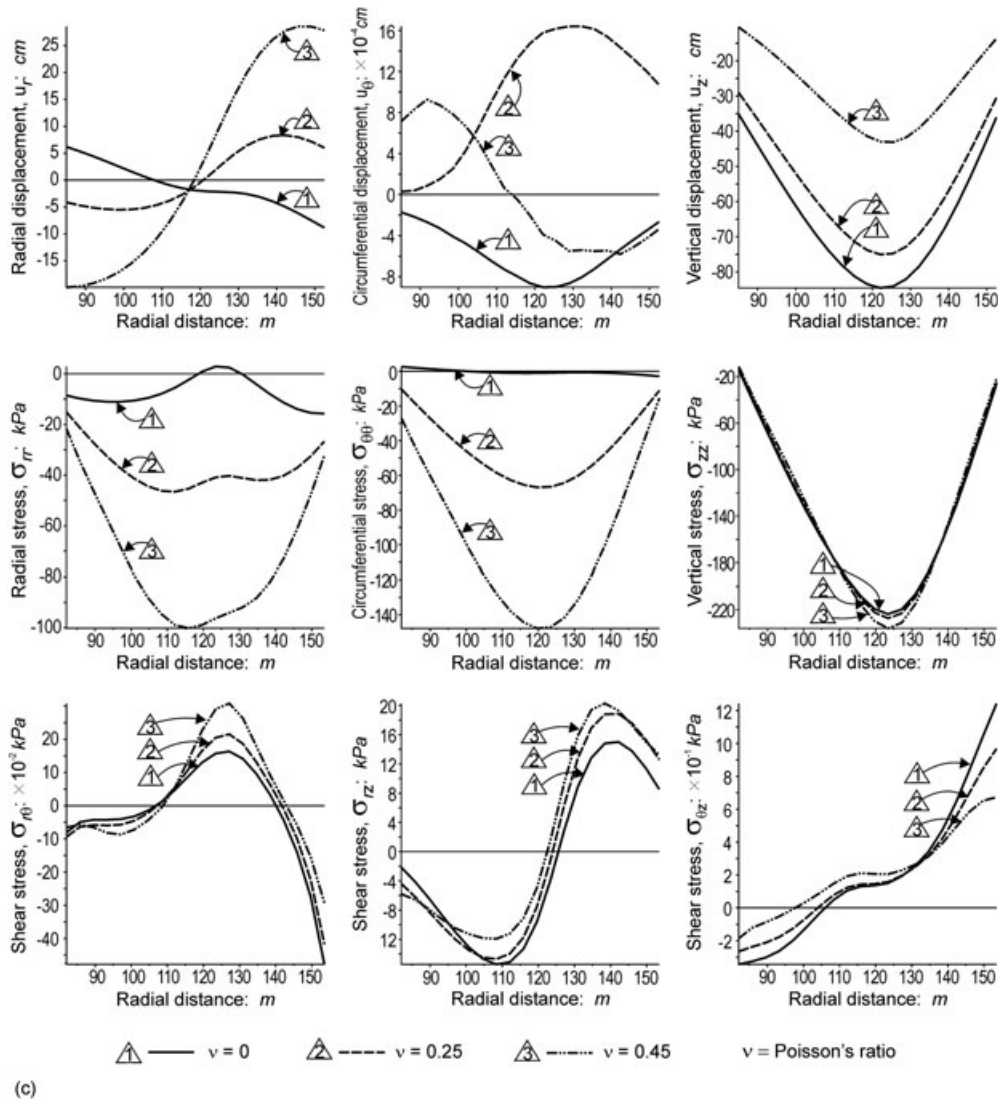


Figure 6. (Continued)

- (a) 2D analysis results are similar to their 3D counterparts, that is, results shown in Figures 8 and 9 are similar. This is taken to affirm correctness of the 3D model results.
- (b) 2D model results in themselves clearly show occurrence of tension zones in the embankment; however, some of the details are more explicit in the 3D model results shown in Figure 8. In part, it could be due to the different contour intervals used in Figures 8 and 9.

Practical significance of the analyses results presented in this section are included in Sections 8 and 9.

7. SAMPLE PROBLEM—SLOPE STABILITY ASSESSMENT

The sample problem shown in Figure 3 was analyzed to determine factor-of-safety against slope failure and the associated slip surface for $R = 5, 23.75, 47.5, 71.25, 95.0,$ and 118.75 m; $R = 5$ m representing a small reservoir and $R = 118.75$ m representing a large reservoir; the dam height was 25 m in all these models. Slope stability analyses were performed in 3D and in 2D axisymmetric modes using the

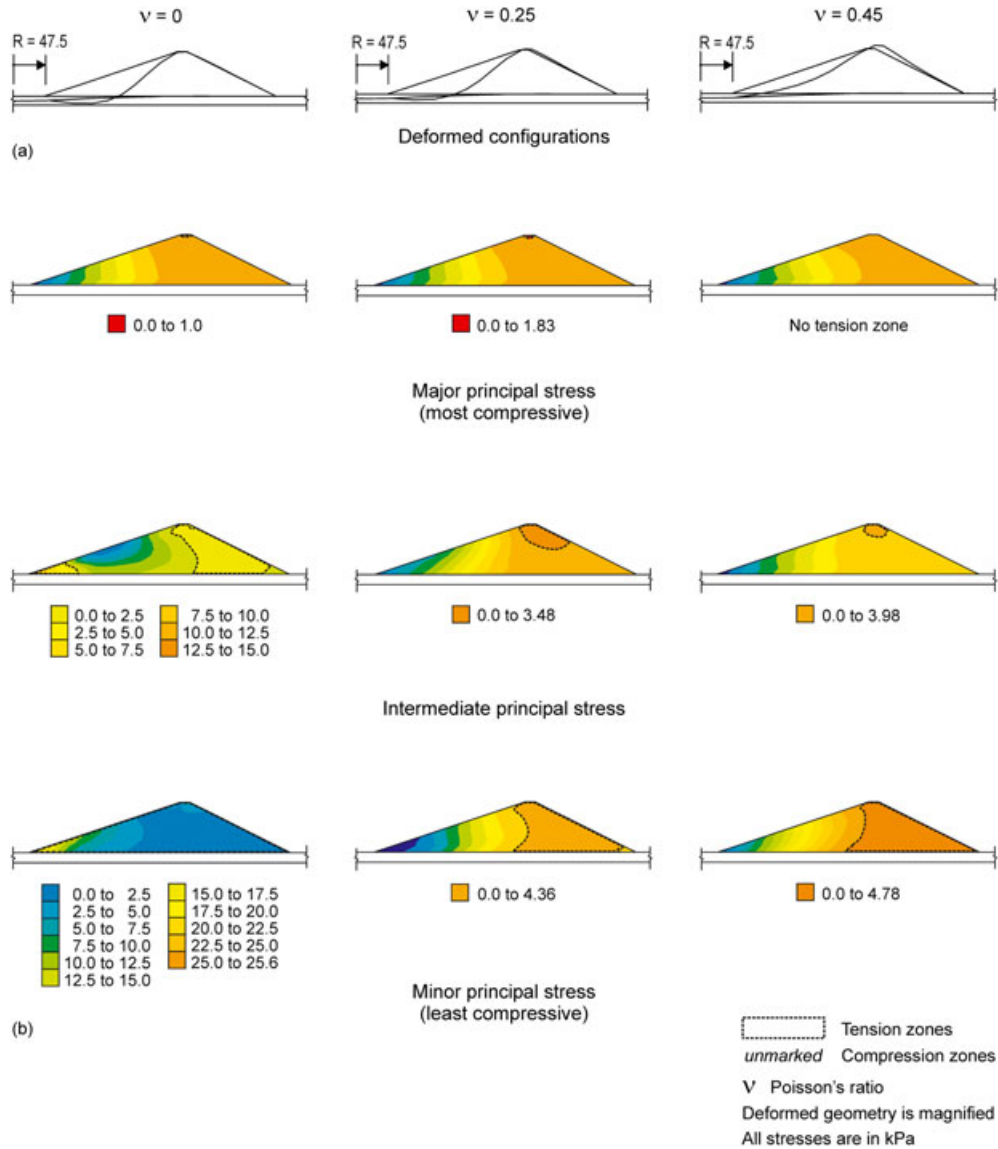


Figure 7. Sample problem (Figure 3); 3D elastic analysis results; loading condition: reservoir water pressure, null self weight, and null pore water pressure, (a) deformed configuration of the dam cross section, (b) principal stresses in the dam cross section, and (c) displacements and stresses in the dam cross section at mid-height of the dam.

computer programs FLAC3D [9] and FLAC [8] for each of the two material property sets shown in Tables I and II.

The computed FoS results for each of the six models with $R=5$ to 118.75 m for the two material property sets are shown in Tables IV and V, respectively. For each material property set, the shear surfaces associated with these FoS are similar; therefore, details of shear surface associated with $R=47.5$ m model only are included herein to conserve space. Figures 10 and 11 show the shear surfaces for the 3D and 2D axisymmetric models, respectively. The failure (slip) surface is along the path of velocity discontinuity, that is, along the interface between the soil mass at rest and the soil mass on the verge of movement. Significant observations from these computed results (FoS and associated shear surface) include the following:

- (a) For each of the two material property sets, 3D factors of safety are somewhat smaller than their counterparts in 2D axisymmetric analyses; in each case, the difference is small (< 5 percent).

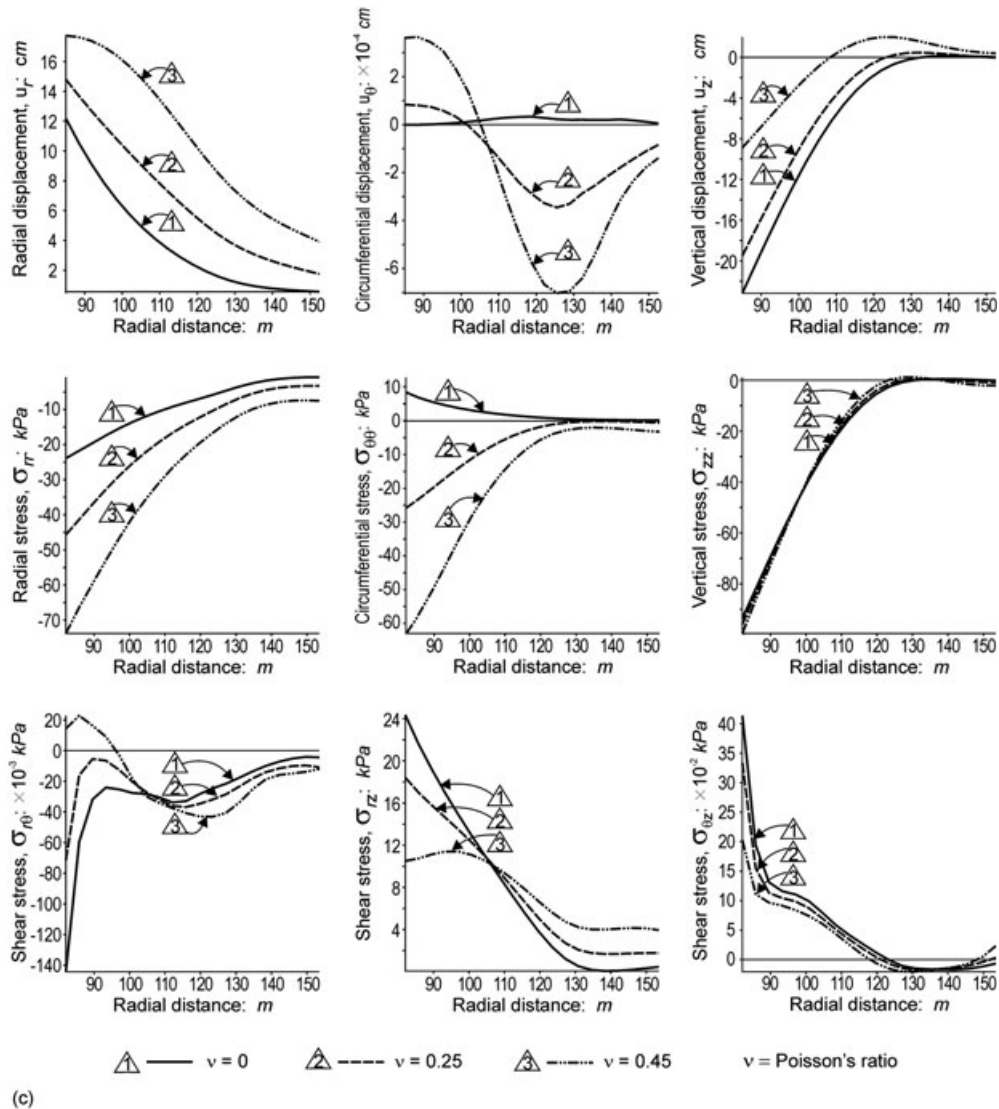


Figure 7. (Continued)

- (b) The size of reservoir did not have a significant effect on the computed FoS.
- (c) For each material property set, the shear surfaces are identical along every radial line.
- (d) The shear surfaces associated with the c, ϕ characterization of the shear strength (Table I) are steeper than their c only (Table II) counterparts.

The 2D model results being higher than their 3D counterparts are interpreted to be caused by differences in the boundary conditions in the hoop direction: the 2D axisymmetric model is relatively more confined in the hoop direction, which results in a higher FoS. For the sample problem, 3D FoS are considered more appropriate than the 2D FoS, although the difference is minimal.

7.1. Effect of Poisson's ratio

The sample problem with $R = 47.5$ m (Figure 3) was analyzed in 2D axisymmetric mode for each of the two material property sets using $\nu = 0$, and 0.25 for Soil_1 (Tables I and II). The FoS and shear surfaces are identical to the ones shown in Tables IV and V and Figure 11. These results are not included herein to conserve space.

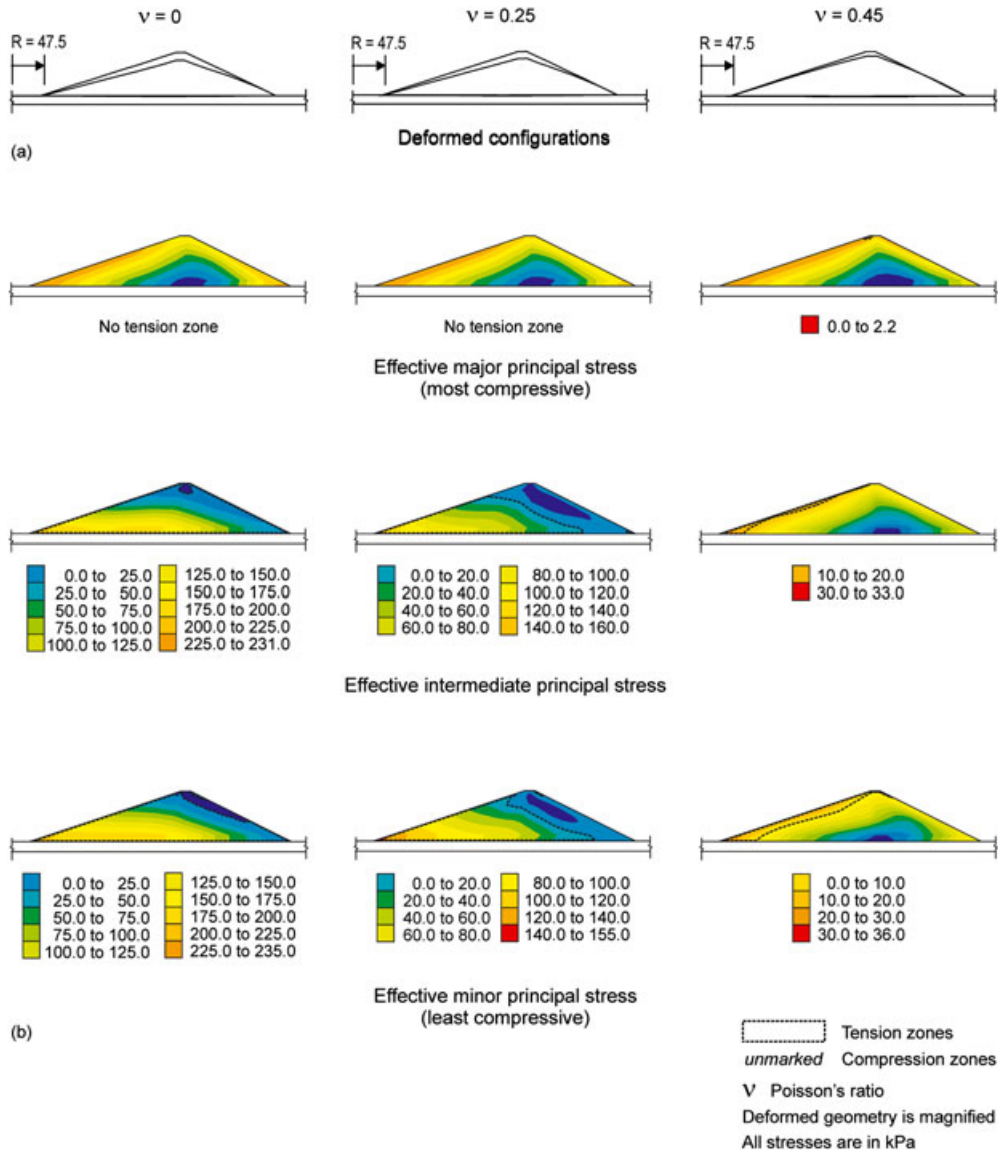


Figure 8. Sample problem (Figure 3); 3D elastic analysis results; loading condition: self weight of the dam, reservoir water pressure, and pore water pressure, (a) deformed configuration of the dam cross section, (b) effective principal stresses in the dam cross section, and (c) displacements and effective component stresses in the dam cross section at mid-height of the dam.

7.2. Effect of weak layer in the dam

Figure 12(a) shows the cross section of the sample problem with a weak layer introduced in the dam. The weak layer is from elevations 87.5 to 90.625 m. Material properties for the weak layer are shown in Table VI. The problem was analyzed for $R=47.5$ m using the 3D model shown in Figure 3.

The computed FoS results for each of the two material property sets with the weak layer included are shown in Table VII, and the shear surfaces associated with the FoS results are shown in Figures 12(b) and 12(c), respectively.

Significant observations from these results include the following:

- (a) For each of the two material property sets, the presence of a weak layer in the dam did not significantly affect the FoS or the shear surface geometry.

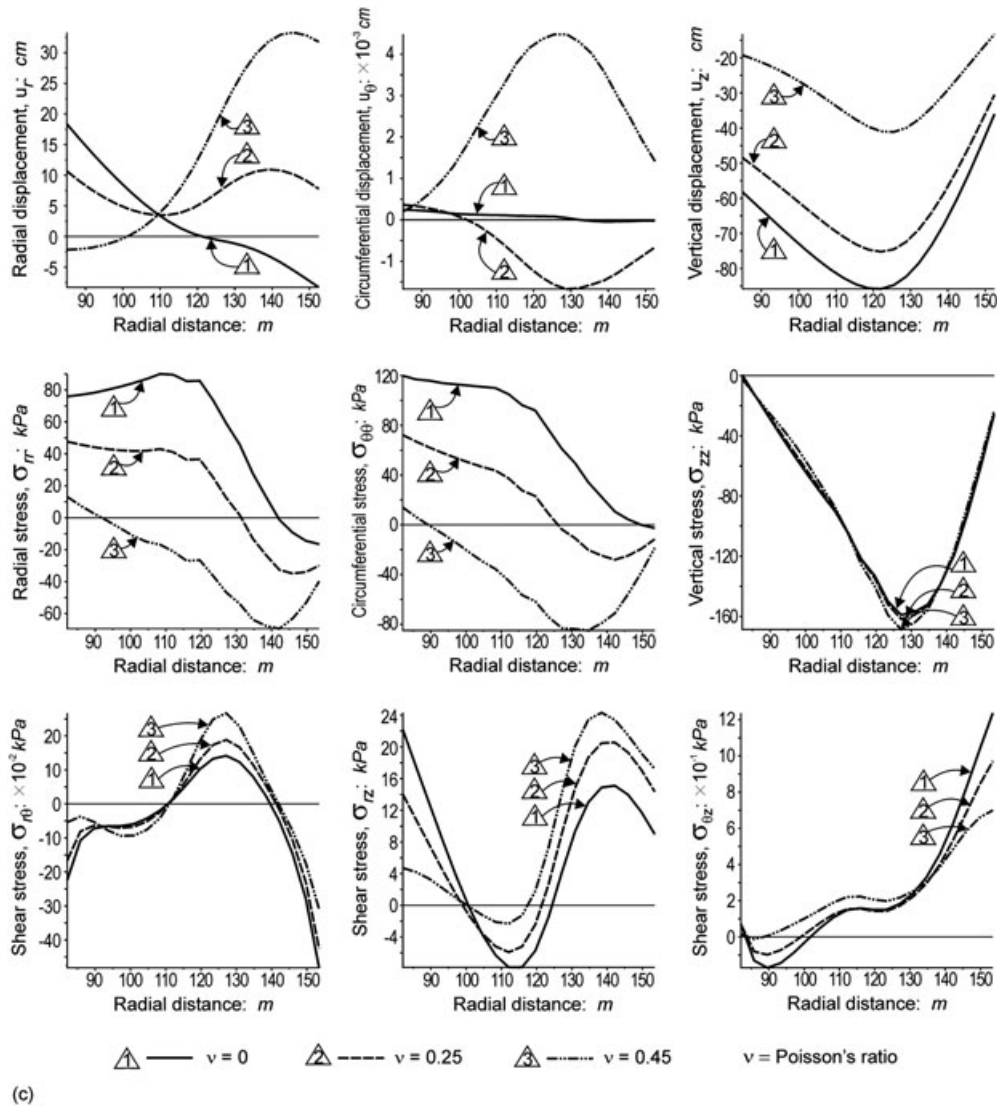


Figure 8. (Continued)

This result is interpreted to imply that the circular geometry of the dam is able to bridge-over local weaknesses in the dam body. However, this inference should be validated by additional analyses.

7.3. Effect of weak layer in the foundation

Figure 13(a) shows the cross section of the sample problem with two weak layers in the foundation block. The thickness of the foundation block is increased to 15 m—the bottom of the model is set at elevation 60 m, and the dam foundation contact is kept at elevation 75 m. Material properties for the weak foundation layers are shown in Table VI. The problem was analyzed for $R = 47.5$ m using the 3D model shown in Figure 3.

The computed FoS results for each of the two material property sets with the weak layer included are shown in Table VII, and the shear surfaces associated with the FoS results are shown in Figures 13(b) and 13(c), respectively.

Significant observations from these results include the following:

- (a) For each of the two material property sets, the presence of weak layers in the foundation has a significant effect on the computed FoS; however, the associated shear surface through the dam

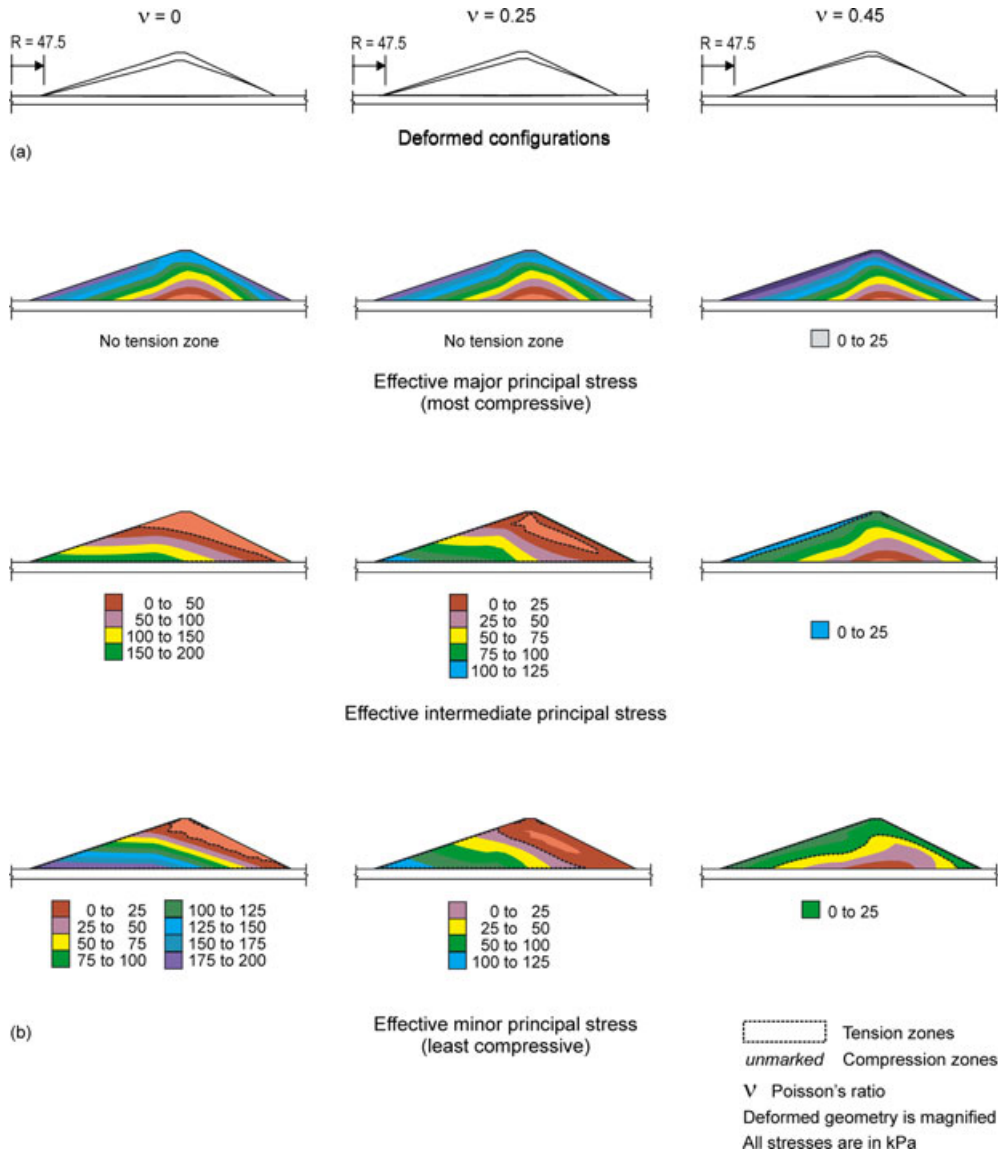


Figure 9. Sample problem (Figure 3); 2D elastic analysis results; loading condition: self weight of the dam, reservoir water pressure, and pore water pressure, (a) deformed configuration of the dam, (b) effective principal stresses in the dam cross section, and (c) displacements and effective component stresses in the dam cross section at mid-height of the dam.

are similar in shape to their counterparts without a weak layer in the dam or foundation, Figures 10 and 11.

This result is interpreted to imply that for the circular dam geometry, presence of weak layers in the foundation is significantly more damaging than their counterparts in the dam body. A more important inference of this result is that foundation material properties (shear strength) need to be known accurately for reliable results from slope stability analyses.

Practical significance of the analyses results presented in this section are included in Sections 8 and 9.

8. IMPLICATIONS IN ENGINEERING PRACTICE

- (a) Most stability assessments of earth dams are performed in terms of FoS and shear surface geometry and location. It is suggested that stability assessments should also include assessments for tension

STABILITY ASSESSMENT OF A CIRCULAR EARTH DAM

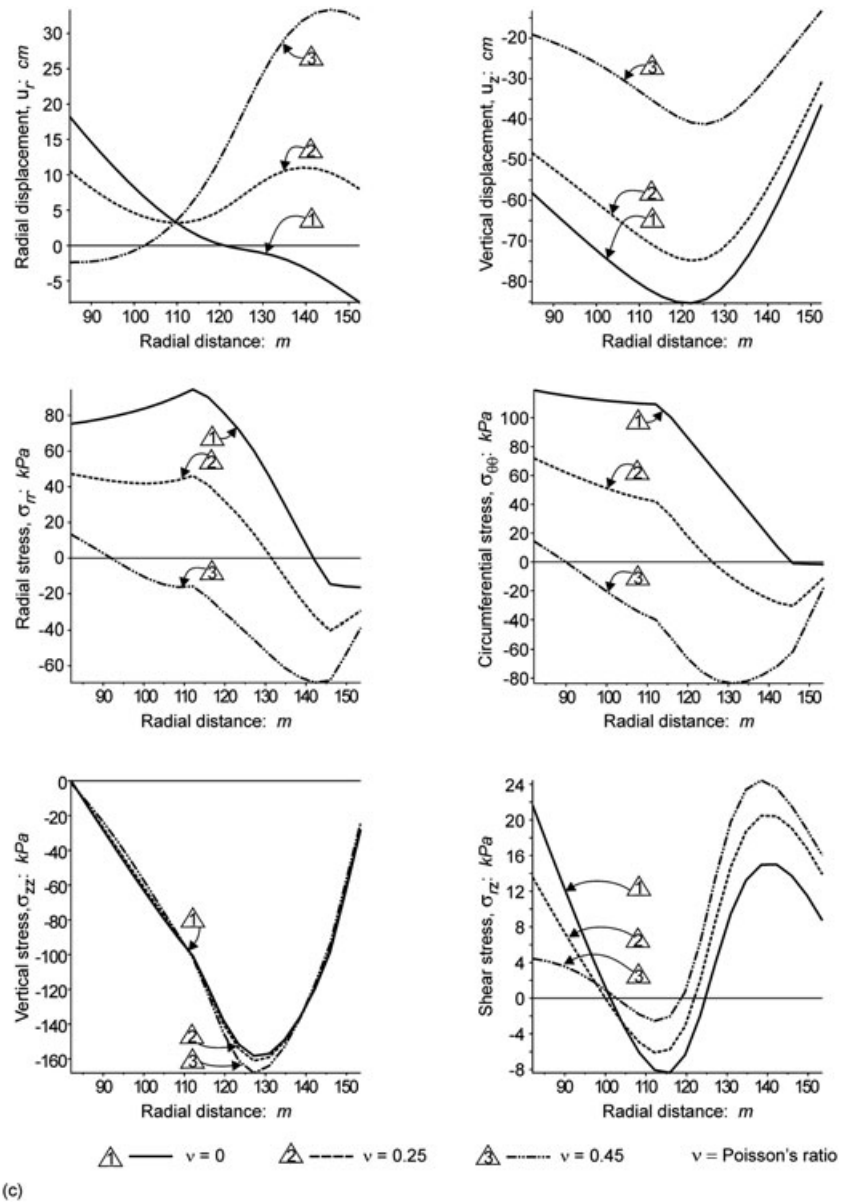


Figure 9. (Continued)

Table IV. Computed factor of safety: material property set no. 1 (Table I).

Sample problem geometry		3D factor-of- safety	2D factor-of-safety
Inside toe distance, R	Dam crest ζ radius		
m	m	FLAC3D	FLAC
5.0	82.50	2.00	2.03
23.75	101.25	1.99	2.03
47.50	125.00	1.96	2.02
71.25	148.75	1.96	2.02
95.00	172.50	1.96	2.02
118.75	196.25	1.95	2.02

Table V. Computed factor of safety: material property set no. 2 (Table II).

Sample problem geometry		3D factor-of- safety	2D factor-of-safety
Inside toe distance, R	Dam crest \mathcal{C} radius		
m	m	FLAC3D	FLAC
5.0	82.50	1.38	1.40
23.75	101.25	1.38	1.39
47.50	125.00	1.37	1.38
71.25	148.75	1.37	1.38
95.00	172.50	1.36	1.37
118.75	196.25	1.36	1.37

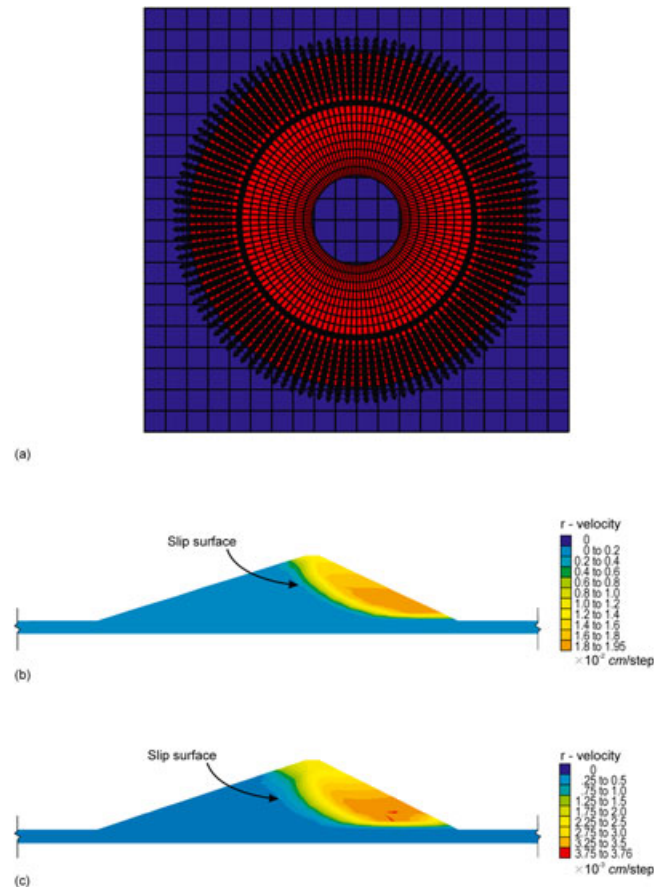


Figure 10. Sample problem (Figure 3); 3D slope stability analysis results; loading condition: self weight of the dam, reservoir water pressure, and pore water pressure, (a) failure surface geometry pattern (typical), (b) failure surface geometry for material property set no. 1, Table I, (c) failure surface geometry for material property set no. 2, Table II.

zones in the dam. It is a simple analysis and can provide valuable insights into a significantly important aspect of dam design, which is location(s) for properly designed and well-constructed protective filters to counter ill effects of seepage-related issues.

- (b) Assessments of tension zones based on the assumption of linear elasticity for all materials in the dam are reliable indicators of where cracks are likely to occur [7].
- (c) Knowing the location and extent of tension zones in a dam, an instrumentation design engineer can decide on an effective instrumentation of the dam and in the interpretation of the field measurements.

STABILITY ASSESSMENT OF A CIRCULAR EARTH DAM

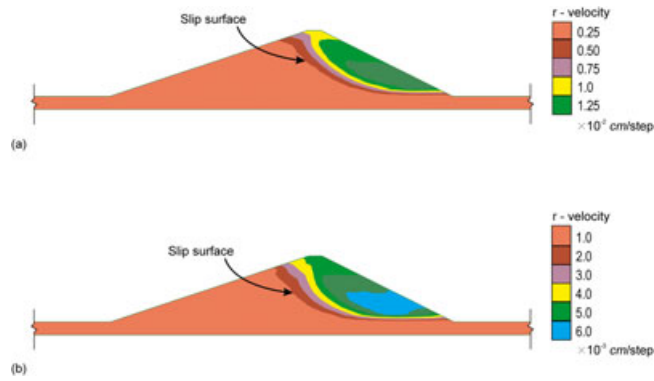


Figure 11. Sample problem (Figure 3); 2D axisymmetric slope stability analysis results; loading condition: self weight of the dam, reservoir water pressure, and pore water pressure, (a) failure surface geometry for material property set no. 1, Table I, and (b) failure surface geometry for material property set no. 2, Table II.

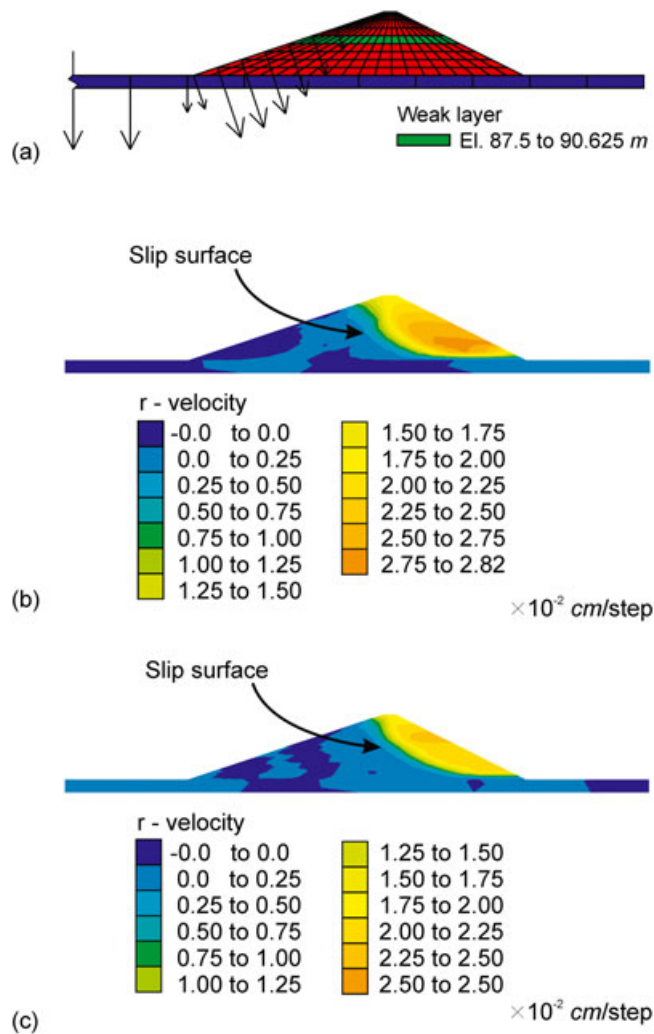


Figure 12. Sample problem (Figure 3) with a weak layer in the dam; 3D slope stability analysis results; loading condition: self weight of the dam, reservoir water pressure, and pore water pressure, (a) cross section view, (b) failure surface geometry for material property set no. 1, Table I, (c) failure surface geometry for material property set no. 2, Table II.

Table VI. Material properties for weak layers: material property set no. 3 (in combination with Table I and Table II data).

Material	Density	Material strength		Elastic constants	
	ρ (kg/m ³)	c' (kPa)	ϕ' (°)	Bulk modulus (kPa)	Shear modulus (kPa)
Table I Elev. 87.5–90.625	1850	10	20	1.67×10^4	1.72×10^3
Table II Elev. 87.5–90.625	1850	35*	0	1.67×10^4	1.72×10^3
Soil_2 Elev. 63–66	1850	70	15	1.33×10^4	1.38×10^3
Soil_2 Elev. 66–75	1850	10	20	1.67×10^4	1.72×10^3

Unit weight γ (N/m³) = Density \times 9.81; for locations of weak layers, see Figures 12 and 13.

*Undrained shear strength.

Table VII. Computed factor of safety; material property set no. 3 (Table VI).

Sample problem geometry:	Weak layer in soil_1		Weak layer in soil_2	
Inside toe distance, R = 47.50 m	Table I	Table II	Table I	Table II
Dam crest ϕ radius = 125.00 m				
3D factor-of-safety FLAC3D	1.87	1.31	1.07	1.00

- (d) It is suggested that 3D numerical analysis of models (based on site-specific conditions) should be performed when and where conditions warrant, for example, near the ends of an earth dam where abutment slopes have a significant effect on the stress regime in the dam. For a circular dam, there are no abutments. However, field conditions are seldom, if ever, completely symmetric; therefore, a 3D analysis for a circular dam should be a preferred choice.
- (e) Reliance on pre-conceived adjustment factors (such as 10–50 percent improvement in FoS) based on simple approximate rules (such as valley width to dam height ratio) for earth dams is not advised. On the contrary, a site-specific slope stability assessment is considered advisable. It takes a little longer to analyze a 3D model as compared with its 2D counterpart, but the added information is helpful in making important design decisions, which have economic payback potential, in addition to giving added confidence in the safe performance of the dam under service conditions. For a circular dam, no approximate rules such as valley width to dam height are suggested in this paper.
- (f) Proper understanding and appreciation of the boundary conditions is advised. For a full 3D model, the boundary conditions are based on physics of the problem, that is, only the bottom and sides of the foundation have displacement restraints (fixed). In a 2D axisymmetric model, one needs to decide on the boundary conditions for the boundary planes at $\theta = \pm$ of the unit radian sector. For example, for the circular geometry, there are two 2D formulations: (i) a 2D plane strain axisymmetric formulation (i.e., hoop strain = 0), and (ii) a 2D plane stress axisymmetric formulation (i.e., hoop stress = 0). The results of these two formulations are not the same among themselves, and neither is equal to no constraint in the hoop direction for the complete model. For the circular dam, neither hoop stress nor hoop strain is null.
- (g) It is not possible to analyze a complete model of a circular dam using available limit equilibrium-based software. However, a 2D axisymmetric model can be used as a substitute; this will have the limitations described in item (f).

9. GENERAL COMMENTS

- (a) Necessary and sufficient checks were exercised to assure credibility in the computed results for the sample problem. These checks were in the form of the following: (i) comparisons of numerical and

STABILITY ASSESSMENT OF A CIRCULAR EARTH DAM

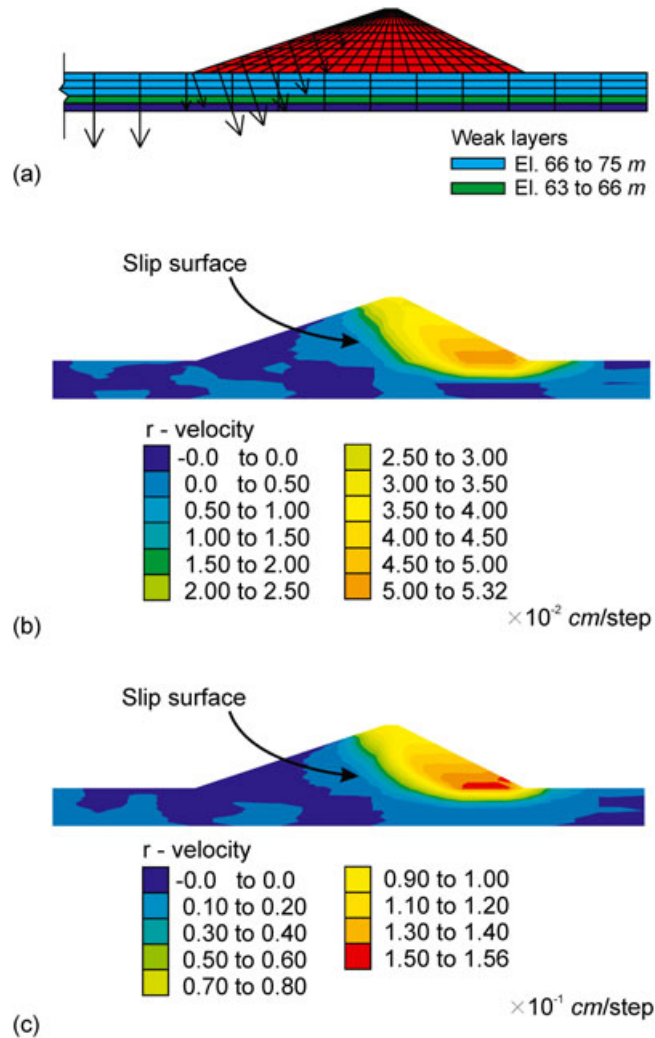


Figure 13. Sample problem (Figure 3) with weak layers in the foundation; 3D slope stability analysis results; loading condition: self weight of the dam, reservoir water pressure, and pore water pressure, (a) cross section view, (b) failure surface geometry for material property set no. 1, Table I, (c) failure surface geometry for material property set no. 2, Table II.

- analytical model results for a test problem of circular water tank; (ii) good agreement of the results with the general expectations regarding location and extension of tension zones under self weight of a homogeneous dam with similar characteristics included in reference [7]; and (iii) consistency of computed results along radial lines including slope stability results (shear surface).
- (b) An element of soil in an embankment is subjected to three principal stresses acting on three mutually perpendicular planes. A tension zone implies that one or more of the three effective principal stresses in that zone is tensile (i.e., +ve by the sign convention).
 - (c) In an earth dam, it is difficult to completely prevent cracks from forming; consequently, there is an increased emphasis on the design of defensive measures to cope with the effects of cracks. For a circular dam with an impervious liner, it is important to have a robust liner, which is free of tears or other imperfections that compromise its effectiveness. For a circular dam without an impervious liner, it is important to have adequate defense(s) against cracking, such as protective filters to inhibit internal erosion caused by concentrated leaks in the dam.
 - (d) Development of a tension crack in a tension zone depends on the magnitude of tensile stress and the tensile strength considered appropriate for the material in the tension zone. No such assessment is included in this paper.

- (e) 3D analyses of the sample problem were performed using symmetric models shown in Figure 2 (b–d). Results obtained were essentially identical to the ones obtained using the complete model, Figure 2(a). The results presented in this paper are from analyses performed on the complete model, Figure 2(a), and 2D axisymmetric model, Figure 2(e).
- (f) Estimates of 10–50 percent improvement in 2D FoS because of 3D geometry are not supported by the results for the circular earth dam. For the sample problem, 3D FoS are somewhat smaller than their counterparts in 2D axisymmetric analyses; in each case, the difference is less than 5 percent.
- (g) Poisson's ratio in the range of 0.25 to 0.45 is typically used in engineering analysis of earth structures. In this paper, $\nu=0$ was primarily for comparison of numerical model results with the analytical results for the circular water tank, which are based on null value for ν . For the sample problem, results for $\nu=0.0, 0.25,$ and 0.45 provide a scale to estimate the sensitivity of results to this parameter.
- (h) Selection of 3D models for the circular earth dam was motivated because of uncertainties in the effects of plane strain b.c. in 2D axisymmetric analysis. For a circular water tank, out-of-plane strain $(\epsilon_{\theta\theta}) = u_r/R$.
- (i) A circular reservoir created via a circular earth dam (parent dam) cannot be partitioned into two semicircular reservoirs by constructing an earth dam along one of the diameters because at the ends of the partitioning dam, the junction will be in constant state of tension because of the radial water pressure on the parent dam. Thus, a circular reservoir can be partitioned only by two concentric ring dams.

10. CONCLUSIONS

- (a) A continuum mechanics-based elastic analysis of an earth dam provides an effective and efficient means to identify location and extent of tension zones in the dam. This information can be used in interpretation of field instrumentation data for existing dams. For new dams, the results can be used to (i) assess merits of different design alternatives in terms of development of tension zones; and (ii) design effective defense(s) against cracking, such as impervious lining to prevent seepage through the dam or protective filters for an unlined embankment.
- (b) Poisson's ratio is an important parameter for determining location and extent of tension zones in a circular earth dam. Young's modulus is an important parameter in determining magnitude of tensile stresses in tension zones but not in determining location or extent of tension zones. Slope stability analysis results—factor-of-safety and shear surface geometry—are not affected by Poisson's ratio.
- (c) For significant projects, 3D stress and stability analyses of an earth dam are suggested. For the sample problem, 3D FoS is actually lower than the corresponding 2D FoS. Thus, estimates of 10 to 50 percent improvement in 2D FoS because of 3D geometry are not supported by the results for a circular earth dam.
- (d) Field conditions are invariably asymmetric (non-symmetric), and it is useful to have a fully functional 3D model for analysis using field data and for what-if scenarios that are considered important for a dam site. However, for an all inclusive symmetric condition, a 2D axisymmetric analysis of a unit radian sector model for a circular dam should suffice—it is only for an ideal situation, which is not likely to be encountered under field conditions.

ACKNOWLEDGEMENTS

The author would like to express his sincere thanks to Professors D. Vaughan Griffiths, Oldrich Hungr, Piaras Kelly, Joseph F. Labuz, Paul A. Martin, Timothy D. Stark, and Dr Zorica Radakovic-Guzina for their interest and helpful communications on the subject matter of this paper.

REFERENCES

1. Sherard JL, Woodward RJ, Gizienski SF, Clevenger WA. *Earth and Earth-Rock Dams*. John Wiley and Sons, Inc.: New York, 1963.
2. Kelly P. *Solid Mechanics Lecture notes*. Department of Engineering Science, University of Auckland: NZ, 2012.
3. Timoshenko S. *Strength of Materials, Part II: Advanced Theory and Problems*. D. Van Nostrand Company: Princeton, 1958.
4. Manning GP. *Reinforced concrete reservoirs and tanks*. Cement and Concrete Association: London, 1972.
5. Reissner H. Ueber die Spannungsverteilung in zylindrischen Behälterwänden. *Beton und Eisen* 1908; **7**:150–155.
6. Sherard JL. *Embankment Dam Cracking. Embankment-Dam Engineering – Casagrande Volume*. John Wiley and Sons, Inc: New York, 1973.
7. Covarrubias SW. Cracking of Earth and Rockfill Dams – a theoretical investigation by means of the finite element method. Contract Report S-69-5. U.S. Army Engineer Waterways Experiment Station, Vicksburg, Mississippi, 1969.
8. Itasca Consulting Group. *FLAC – Fast Lagrangian Analysis of Continua*. Itasca Consulting Group, Minneapolis, Minnesota, 2006.
9. Itasca Consulting Group. *FLAC3D – Fast Lagrangian Analysis of Continua in 3 Dimensions*. Itasca Consulting Group, Minneapolis, Minnesota, 2002.
10. Hungr O, Wilson P. Stability of slopes curved in plan – an example. In proceedings of the 59th Canadian Geotechnical Conference, Vancouver, British Columbia, October 2006.
11. Adriano PRR, Fernandes JH, Gitirana GFN, Fredlund MD. *Influence of ground surface shape and Poisson's ratio on three-dimensional factor of safety*. GeoEdmonton '08: 61st Canadian Geotechnical Conference Proceedings, Edmonton, Alberta September 2008.
12. Inci G. 3D effects on flood protection levees – plain strain versus axisymmetric modelling. In proceedings of the 12th International Conference of International Association for Computer Methods and Advances in Geomechanics, Goa, October 2008.
13. Ormann L, Zardari MA, Mattsson H, Bjelkevik A, Knutsson S. Numerical analysis of curved embankment of an upstream tailings dam. *Electronic Journal of Geotechnical Engineering* 2011; **16**(1):931–944.
14. Chugh AK, Stark TD. An automated procedure for 3-dimensional mesh generation. In proceedings of the 3rd International Symposium on FLAC and FLAC3D Numerical Modelling in Geomechanics, Sudbury, Ontario, October 2003.
15. Timoshenko S, Woinowsky-Krieger S. *Theory of Plates and Shells*. McGraw-Hill Book Company: New York, 1959.